

# Mechanism of determination of the shedding frequency of vortices behind a cylinder at low Reynolds numbers

By MICHIO NISHIOKA

College of Engineering, University of Osaka Prefecture, Japan

AND HIROSHI SATO

Institute of Space and Aeronautical Science,  
University of Tokyo, Japan

(Received 9 December 1977)

Two kinds of experiment were made in the wake of a cylinder at Reynolds numbers ranging between 20 and 150. One was a close look at the structure of the vortex street with a stationary cylinder at Reynolds numbers greater than 48. The other experiment was made at lower Reynolds numbers with a cylinder vibrating normal to the flow direction. In this case an artificially induced small-amplitude fluctuation grows exponentially with the rate predicted by the stability theory. Because of the similarity between the two kinds of wake, we postulate that the shedding of the vortex at low Reynolds numbers is initiated by the linear growth, namely, the fluctuation with the frequency of maximum linear growth rate develops into vortex streets. By using the measured width of the wake at the stagnation point in the wake and the result of the stability theory, we could calculate the Strouhal number for Reynolds numbers ranging from 48 to 120. The predicted Strouhal numbers agree well with the values from direct measurements.

---

## 1. Introduction

Although there are many investigations on the vortex shedding from a cylinder, the mechanism by which the shedding frequency is determined is not yet clear. In other words, the empirical relation between the shedding frequency and Reynolds number established by Roshko (1954) and other investigators has not been adequately explained. There are many approaches to the problem. One is to use the vortex model. The roll-up of the shear layer separated from the surface of the cylinder results in the formation of the vortex street. When the Reynolds number is sufficiently high, the roll-up takes place alternately at both sides of the cylinder and vortices are shed alternately into the wake. The geometrical arrangement of the vortices is determined by von Kármán's theory. If we make detailed experiments, however, we find that the ratio of longitudinal to lateral spacings of the vortex street is different from von Kármán's value. Moreover, the shedding frequency is not determined by this model.

Another approach is the use of the linear or nonlinear stability theory. The linear stability theory of shear flows predicts growth rates of small-amplitude fluctuations. Among fluctuations with various frequencies there is a fluctuation of the maximum growth rate. In fact, in the wake behind a thin flat plate placed parallel to the flow a small-amplitude fluctuation grows exponentially and the frequency of the fluctuation

existing in the wake corresponds to that of the maximum growth rate due to the linear stability theory (Sato & Kuriki 1961; Mattingly & Criminale 1972). In experiments behind a cylinder at high Reynolds number, however, exponential growth of the fluctuation has not been found. In fact, the sinusoidal fluctuation in the wake decays downstream. Therefore, the shedding frequency cannot be determined by the linear theory. The formation of the vortex street is a nonlinear closed process which has a very sharp selectivity in the frequency. This process includes a strong interaction between the mean-velocity field and the fluctuation.

The vortex street is not formed at Reynolds numbers below about 40. By introducing an artificial disturbance into the wake at Reynolds numbers slightly below 40 we may be able to observe the growth of the disturbance, which may eventually lead to the formation of an artificial vortex street. If this process really occurs, we may imagine the same process taking place at higher Reynolds numbers. This is the motivation for the present investigation. It is a direct extension of the previous work on the flow around a cylinder at low Reynolds numbers (Nishioka & Sato 1974). It begins with a close look at the mean and fluctuating velocities around the cylinder at low Reynolds numbers. Then the streamwise variations of an artificial disturbance superposed at lower Reynolds numbers is observed. The observed growth rate of the fluctuation is compared with results of the linear stability theory at various Reynolds numbers. The shedding frequency from a stationary cylinder is also compared with these results and the possibility of connecting observed Strouhal numbers with stability theory is investigated.

## 2. Experimental arrangement

The whole experiment was conducted in a suction-type low-speed wind tunnel with a test section of  $20 \times 20$  cm cross-section and 60 cm in length. The wind speed in the test section was varied between 10 and 100 cm/s. The distribution of the mean velocity in the test section was uniform within 2 per cent except in the boundary layers along walls. The residual turbulence in the test section measured by a hot-wire anemometer with a low-cut filter of 8 Hz was about 0.01 per cent at the wind speed 20 cm/s. The turbulence level was the same at 70 cm/s with a low-cut filter of 15 Hz. Measurements of mean and fluctuating velocities were made by a constant-temperature hot-wire anemometer. The hot wire was mounted on a traversing mechanism with an orientation such as to pick up  $u$ -fluctuations. A linearizer was specially designed and constructed for the measurements at wind speeds below 150 cm/s (Nishioka 1973). It was necessary to take into account the deviation from the conventional King's law at these extremely low wind speeds. The calibration of the anemometer was made by the periodic heat-wake method. The method employs two hot wires placed parallel with variable spacing in the direction of flow. The upstream wire is heated by an alternating current of known frequency. The periodic heat wake of the upstream wire is picked up by the downstream wire. By changing the spacing we obtain the wavelength, hence the wind speed. Details of the wind tunnel, the calibration procedure and the problems associated with measurements at low wind speeds are found in the previous paper (Nishioka & Sato 1974).

A Bakelite rod (3.0 mm in diameter) was spanned vertically in the test section and used for the natural vortex shedding experiment. Reynolds numbers,  $R = U_\infty d/\nu$ ,

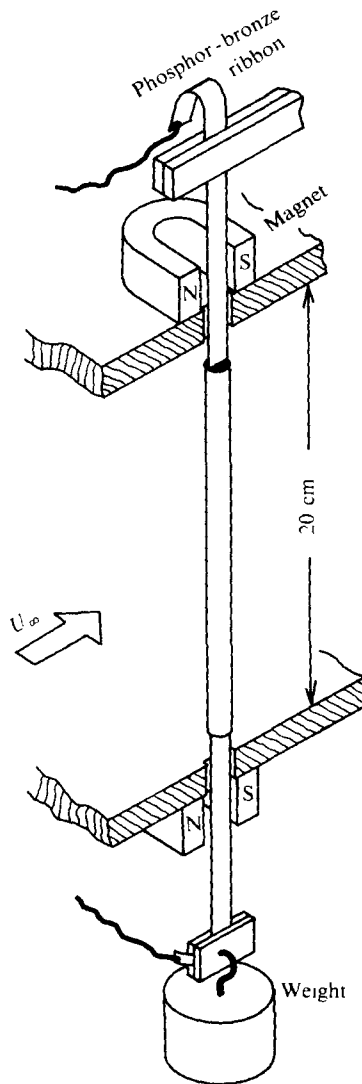


FIGURE 1. Arrangement for experiment with vibrating cylinder.

from 40 to 200 were covered by the use of the rod. The experiment with a forced vibration was made with a plastic pipe with an insertion of thin phosphor-bronze ribbon. A pipe with a diameter of 2.0 mm covers Reynolds numbers between 20 and 40 and a pipe with a diameter of 3.0 mm was used for higher Reynolds numbers. The pipe was 17 cm long. The ribbon protruded from the ceiling and floor of the test section and an adequate tension was given by a weight as shown in figure 1. The pipe was forced to vibrate either parallel or normal to the flow by the electromagnetic force caused by a permanent magnet and an alternating current through the phosphor-bronze ribbon. It was ascertained that the cylinder vibrated with the same amplitude and phase at all points along the axis. The amplitude of vibration was measured by a telescope from outside. The amplitude was varied between 4 and 15 per cent of the diameter.

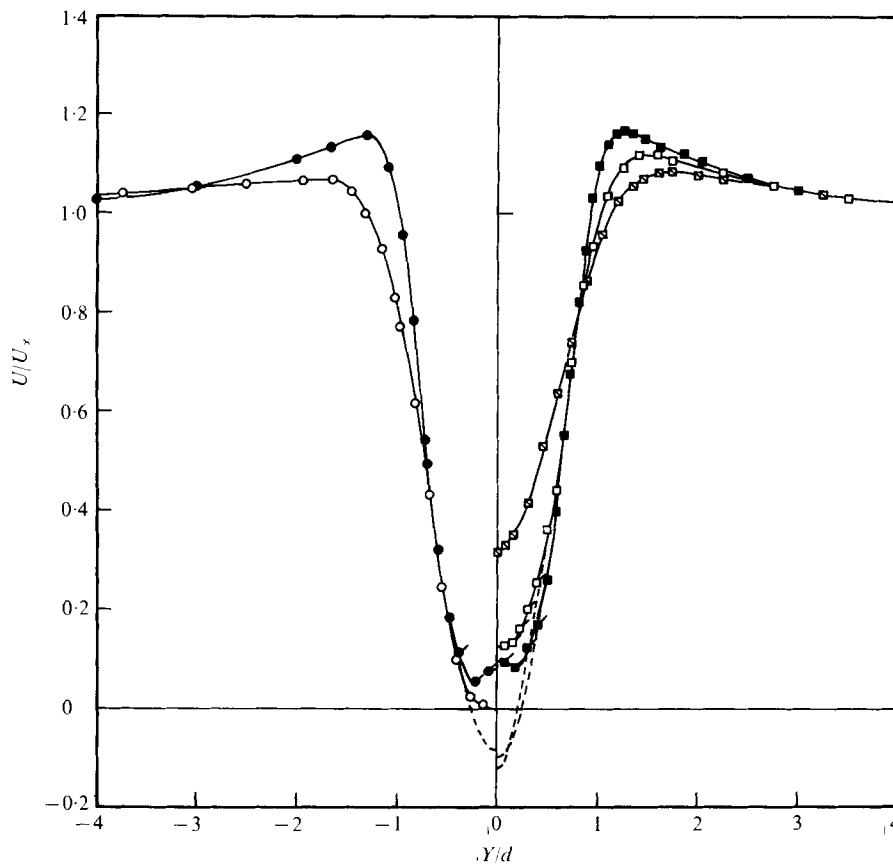


FIGURE 2. Mean-velocity distributions in wake at  $R = 48$  and  $70$ . Left half:  $R = 48$ ;  $\bullet$ ,  $X/d = 1.0$ ;  $\circ$ ,  $X/d = 3.2$ . Right half:  $R = 70$ ;  $\blacksquare$ ,  $X/d = 1.0$ ;  $\square$ ,  $X/d = 1.8$ ;  $\square$  with flag,  $X/d = 3.2$ . Data points with flags are not accurate.

The  $X$  axis is taken in the flow direction, the  $Z$  axis is along the cylinder and the  $Y$  axis is perpendicular to both axes with the origin at the mid-point of the axis of the cylinder.

### 3. Vortex shedding from a stationary cylinder

In the experiment with a stationary cylinder a weak sinusoidal fluctuation was observed near the stagnation point in the wake (the downstream edge of a pair of standing eddies behind the cylinder) when the Reynolds number exceeded 48. The mean velocity distributions in the wake at Reynolds numbers 48 and 70 are illustrated in figure 2. The mean velocity at  $R = 48$  measured at  $X/d = 1$  (inside the standing eddies) shows a non-minimum value on the centre-line. The hot-wire anemometry in the low-speed near wake involves difficult problems, such as the nonlinearity, the rectifying effect, and large variations of flow direction. The linearization was achieved by an analog device as described in Nishioka & Sato (1974). There still remain uncertainties due to the variation of flow direction. Flags on data points in figure 2 indicate that they are not accurate. The actual distributions might be those indicated

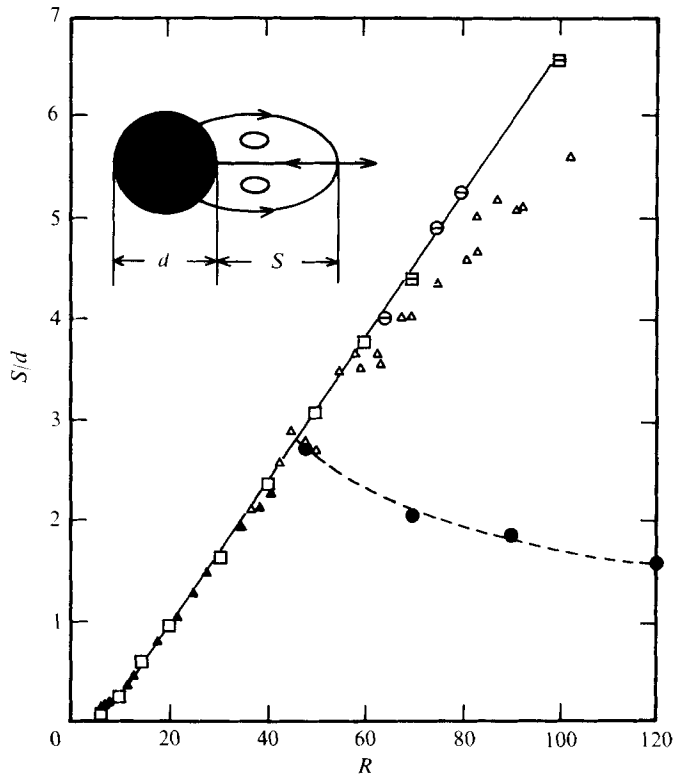


FIGURE 3. Length of eddies behind cylinder *vs.* Reynolds number. Experimental results: ●, present work; ○, Nishioka & Sato; ▲, Taneda; △, Acivos *et al.* Numerical results: □, Takami & Keller; □, Dennis & Chang.

by broken lines. The distribution shows a velocity overshoot between  $|Y/d| = 1$  and 5. This is due to the acceleration at the 'shoulder' of the cylinder. These features are almost the same at  $R = 70$ . Distributions at higher Reynolds numbers up to 200 are alike. The position of the stagnation point was determined by the extrapolation of the centre-line velocities measured at large  $X/d$ . The result is shown in figure 3 together with other theoretical and experimental results. Taneda (1956) showed the existence of standing eddies for Reynolds numbers up to 150 by flow-visualization techniques. The points near the straight line in the figure are results when there is no vortex shedding. On the other hand, the present results with a slight decrease at higher Reynolds numbers are accompanied by the vortex shedding. The shedding is suppressed when the aspect ratio of the cylinder is small. Our previous data (Nishioka & Sato 1974) were obtained with an aspect ratio of 6.5 in contrast to the present experiment with the ratio 67. It is obvious that the formation of the vortex street changes the nature of the wake significantly.

The wave form of the fluctuation in the wake is periodic and steady up to a Reynolds number of 200. The two-dimensionality of the intensity of fluctuation is also good. No difference was found in the  $Y$  distributions of  $\overline{u^2}$  at various  $Z$  stations for  $-8 < Z/d < 10$ . On the other hand, the phase of fluctuation changes in the  $Z$  direction. The phase change in  $Z$  is almost linear. This change suggests the inclination of

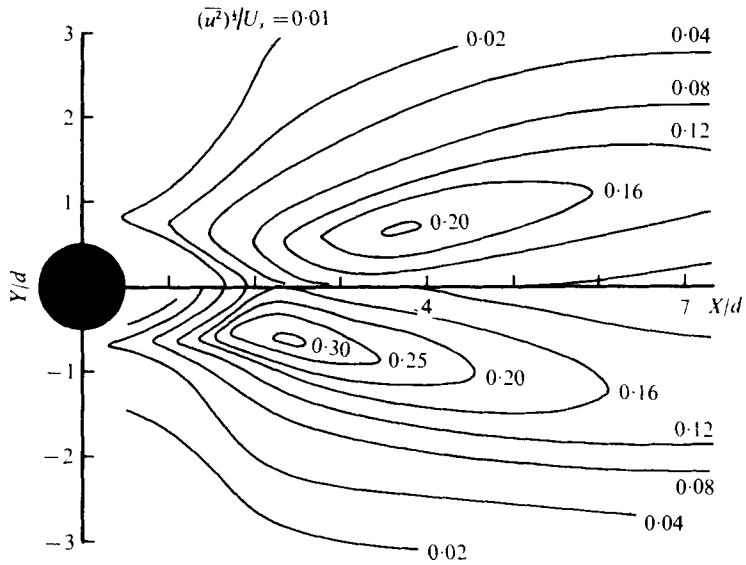


FIGURE 4. Equi-intensity lines of  $u$ -fluctuation at  $R = 70$  (upper half) and 120 (lower half).

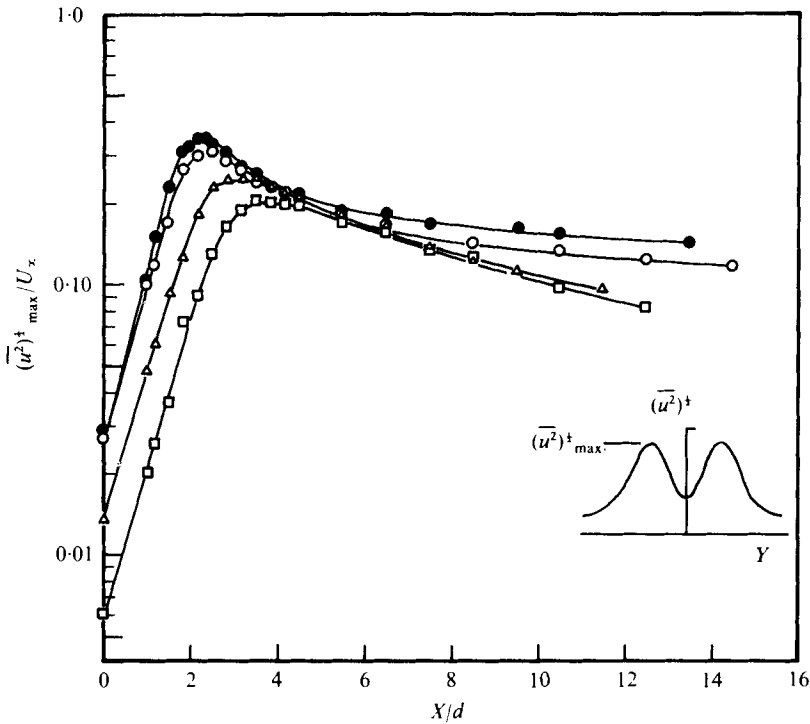


FIGURE 5. Streamwise variations of the maximum fluctuation intensity,  $(\bar{u}^2)^{\dagger}_{max}/U_{\infty}$ :  $\square$ ,  $R = 70$ ;  $\triangle$ ,  $R = 90$ ;  $\circ$ ,  $R = 120$ ;  $\bullet$ ,  $R = 150$ .

vortices in the flow direction. The angle of inclination is about  $17^\circ$ ,  $18^\circ$ ,  $20^\circ$  and  $19^\circ$  at  $R = 63, 90, 120$  and  $150$ , respectively. One possible reason for the inclination is the difference in the flows at both ends of the cylinder.

The equi-intensity lines of the  $u$  fluctuation in the wake are shown in figure 4 for Reynolds numbers 70 and 120. The maximum of the fluctuation amplitude is found at  $X/d = 3.5$  at  $R = 70$  and  $2.3$  at  $R = 120$ . The point of maximum fluctuation moves upstream as the Reynolds number is increased. It is more clearly demonstrated in figure 5, in which the streamwise variation of the maximum of  $(\overline{u^2})^{1/2}$  in the  $Y$  distribution at each  $X$  station is plotted in a semi-logarithmic scale. As the Reynolds number is increased the  $X$  station of maximum  $\overline{u^2}$  moves close to the cylinder and the maximum value increases. At small  $X/d$  the growth is exponential. This exponential growth takes place mostly inside the standing eddies behind the cylinder. The region of the exponential growth becomes narrower at higher Reynolds number. This suggests that at sufficiently high Reynolds numbers the exponential growth does not exist at all in the wake. The growth rates at four Reynolds numbers in figure 5 are almost the same. It must be noted, however, that the amplitude of fluctuation at high Reynolds numbers exceeds 30 per cent at  $X/d = 2$ . They are not 'small' fluctuations and the comparison with the linearized theory is meaningless. At low Reynolds numbers amplitudes are small. The growth seems to be the so-called linear growth when the Reynolds number is below 70.

#### 4. Fluctuations in the wake of a vibrating cylinder

When the cylinder vibrates normal to the flow, a periodic velocity fluctuation is created in the wake. The fluctuation grows or decays in the flow direction. For Reynolds numbers below 20 no growth takes place. For Reynolds numbers above 48 a natural fluctuation appears without forcing. Therefore, the detailed experiment with a vibrating cylinder was made between these two Reynolds numbers. The growth and decay of the fluctuation depend on the amplitude and frequency of the vibration. An example of the effect of the amplitude at  $R = 30$  is shown in figure 6, in which the maximum intensity at each  $X$  station  $(\overline{u^2})^{1/2}_{\max}/U_\infty$  is plotted against  $X/d$ . For small vibration amplitudes,  $a/d = 0.04$  and  $0.08$ , the fluctuation grows almost exponentially at small  $X$ , levels off at around  $X/d = 8$  and decreases further downstream. The rate of exponential growth at small  $X$  is almost the same for two vibration amplitudes. The mean velocity distribution with  $a/d = 0.08$  coincides with that without vibration within 2 per cent close behind the cylinder. For a large amplitude,  $a/d = 0.15$ ,  $(\overline{u^2})^{1/2}_{\max}/U_\infty$  is about 0.05 at  $X/d = 2$  and decreases downstream monotonically. Obviously, if the initial amplitude is too large, the exponential growth does not take place.

The effect of the frequency of the vibration was examined with small vibration amplitudes ( $a/d \leq 0.08$ ), as shown in figure 7. The Reynolds number was 40 and the frequency of vibration was changed from 6 to 25 Hz. If the frequency is between 14 Hz and 20 Hz, the fluctuation grows exponentially. The 9 Hz fluctuation stays almost unchanged and the 6 Hz fluctuation decays. The non-dimensional growth rate  $-\alpha_i$  is calculated from  $-\alpha_i = d \ln [(\overline{u^2})^{1/2}_{\max}/U_\infty]/d(X/b)$  as a function of the non-dimensional frequency,  $\beta = 2\pi fb/U_\infty$ , where  $b$  is the half-value width of the wake. The wavelength in the  $X$  direction,  $\lambda$  was determined by the phase measurement. The

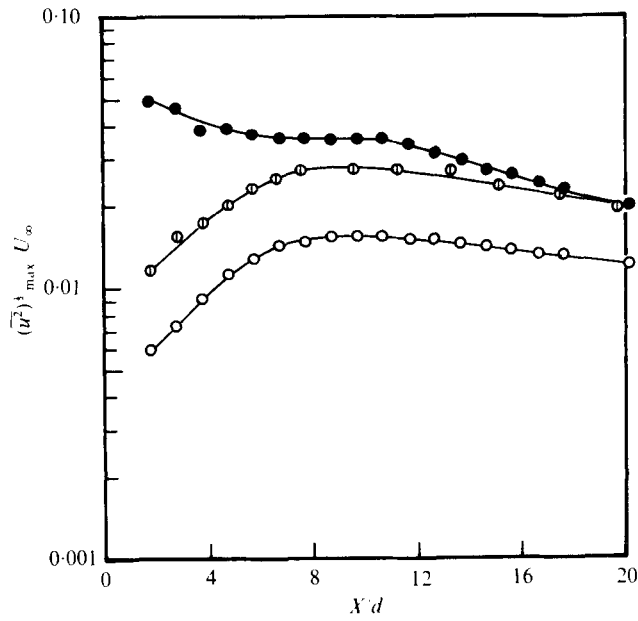


FIGURE 6. The streamwise development of a sinusoidal fluctuation ( $f = 12$  Hz,  $R = 30$ ) with various cylinder amplitudes,  $a/d$ :  $\circ$ ,  $a/d = 0.04$ ;  $\odot$ ,  $a/d = 0.08$ ;  $\bullet$ ,  $a/d = 0.15$ .

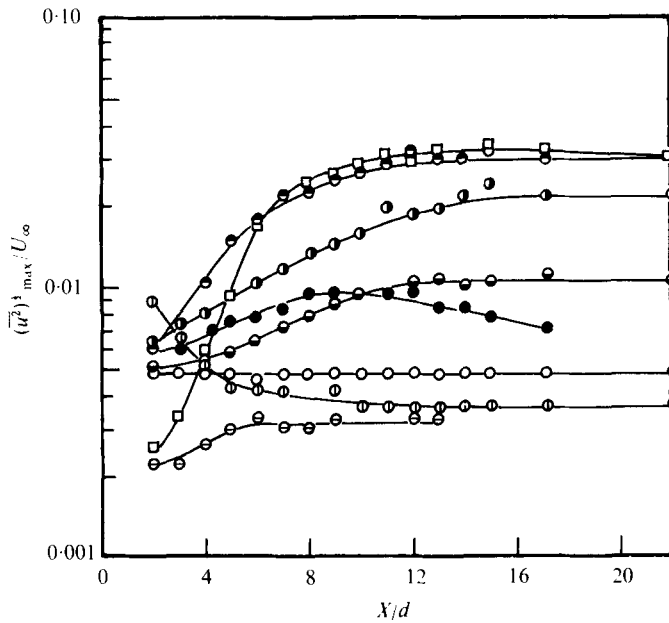


FIGURE 7. Streamwise growth and decay of small fluctuations at  $R = 40$ :  $\odot$ ,  $f = 6$  Hz;  $\circ$ ,  $f = 9$  Hz;  $\ominus$ ,  $f = 10$  Hz;  $\bullet$ ,  $f = 14$  Hz;  $\bullet$ ,  $f = 16$  Hz;  $\bullet$ ,  $f = 18$  Hz;  $\square$ ,  $f = 20$  Hz;  $\bullet$ ,  $f = 25$  Hz.



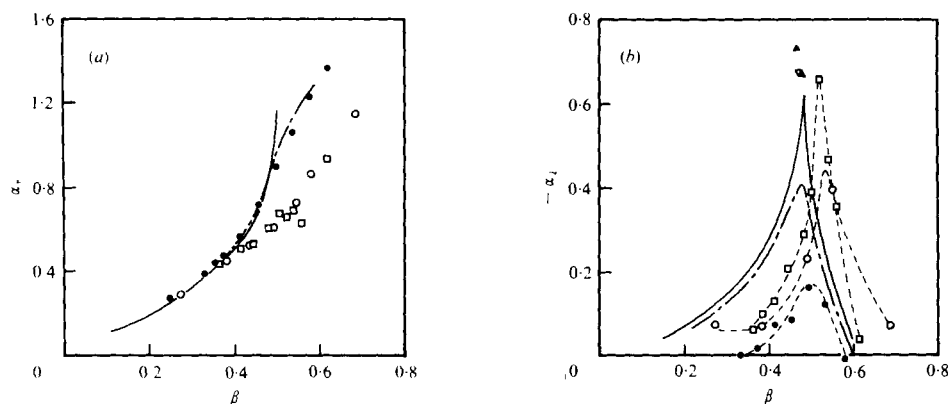


FIGURE 8. Fluctuation eigenvalues. (a) Wavenumber  $\alpha_r$  vs. angular frequency  $\beta$ . (b) Spatial growth rate  $-\alpha_i$  vs. angular frequency,  $\beta$ . Vibrating cylinder:  $\bullet$ ,  $R = 30$ ;  $\circ$ ,  $R = 40$ ;  $\square$ ,  $R = 46.5$ . Natural fluctuation:  $\triangle$ ,  $R = 70$ ;  $\nabla$ ,  $R = 90$ ;  $\blacktriangle$ ,  $R = 120$ . Nakaya's calculations:  $-\cdot-$ ,  $R_b = 30$ ;  $—$ ,  $R_b = 40$ .

non-dimensional wavenumber  $\alpha_r$  is defined as  $2\pi b/\lambda$ . Both  $\alpha_r$  and  $-\alpha_i$  are plotted against  $\beta$  in figures 8(a) and (b). The wavenumber  $\alpha_r$  increases rapidly with  $\beta$  at three Reynolds numbers. The growth rate  $-\alpha_i$  is large for high Reynolds numbers and has a peak at around  $\beta = 0.5$ . The selectivity is sharper at higher Reynolds numbers. In both figures theoretical results on eigenvalues for spatial growth by Nakaya (1976) are added for comparison. In his calculation the velocity on the centre-line is zero and the Reynolds number  $R_b$  is defined by  $U_\infty b/\nu$ . Our measurements show that  $d \approx 1.3b$ , therefore,  $R_b = 30$  and  $40$  correspond roughly to  $R = 40$  and  $50$ , respectively. The agreement between experimental and theoretical results is good, for both  $\alpha_r$  and  $-\alpha_i$ . There is about 10 per cent discrepancy for  $\beta$  with maximum growth rate [figure 8(b)]. This may be attributed to a slight difference in experimental and theoretical mean velocity distributions.

Distributions of the amplitude and phase of  $u$  fluctuations at two different Reynolds numbers are shown in figure 9. Frequencies of the vibration are 12 Hz and 8.8 Hz at  $R = 30$  and  $46.5$ , respectively. The maximum r.m.s. values are about  $0.01U_\infty$  in both cases. Distributions of the amplitude at two different Reynolds numbers are almost the same with two maxima at around  $|Y/d| = 0.5$ . There is a 180 degree phase difference at two symmetrical points with respect to the centre-line. Theoretical curves by Nakaya (1976) are also shown. The agreement between the two results is fairly good.

An experiment with the vibration parallel to the flow was also made at  $R = 30$ . In this case the  $u$  fluctuation is symmetric with respect to the centre-line at  $X/d = 1$  but becomes antisymmetric at  $X/d \geq 3$ . This fact suggests that antisymmetric fluctuations have higher growth rates than symmetric fluctuations. This result agrees with the linear stability theory which predicts larger growth rate for antisymmetric fluctuation. Therefore, only antisymmetric disturbances were examined in detail.

From these experimental results we conclude that in the wake of a vibrating cylinder we can excite sinusoidal fluctuations which grow in the flow direction as

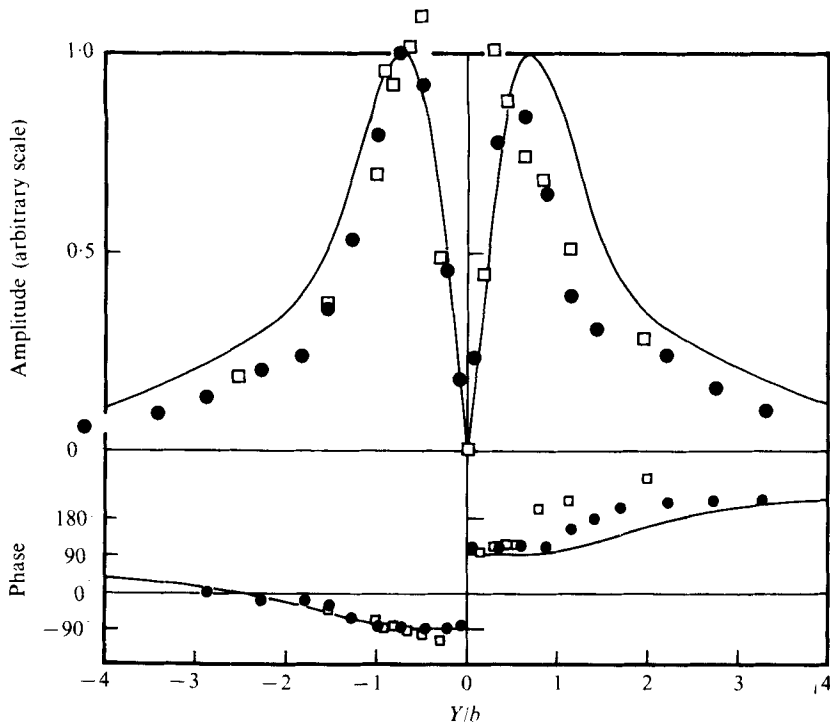


FIGURE 9. Distributions of amplitude and phase of sinusoidal fluctuations. Experimental conditions ( $R$ ,  $d$ ,  $X/d$ ,  $f$ ): ●, (30, 2.0 mm, 5, 12 Hz); □, (46.5, 3.0 mm, 2.5, 8.8 Hz). Full lines represent theoretical results of Nakaya;  $R_b = 40$ ,  $\beta = 0.48$ .

predicted by the linear stability theory, and form a vortex street behind the cylinder similar to the one at higher Reynolds numbers.

### 5. Mechanism of determining shedding frequency

In the experiment with a stationary cylinder sinusoidal fluctuations were observed in the wake when the Reynolds number exceeded 48. This critical Reynolds number is a little higher than the value 40 which is generally accepted. One possible reason for the higher value is the low residual turbulence in the test section of the present experiment. If the turbulence is reduced further, the critical Reynolds number may become higher. In the experiment with a vibrating cylinder at Reynolds numbers between 20 and 48 we observed the exponential growth of the sinusoidal velocity fluctuation, which developed into a vortex street. The growth is selective, in other words, fluctuations in a certain frequency range grow. The non-dimensional frequency for maximum growth is around  $\beta_m = 0.5$  as shown in figure 8. We can calculate a fictitious Strouhal number at Reynolds numbers between 20 and 48 by the relation  $St = fd/U_\infty = \beta_m(d/2\pi b)$ . If we use the experimental value of  $d/b$  and Nakaya's theoretical value 0.48 for  $\beta_m$ , we obtain  $St = 0.1$ .

We extend the calculation to higher Reynolds numbers for which natural vortex shedding takes place. In this case  $b$  changes in the flow direction. So we take  $b$  at the  $X$  station of the stagnation point in the wake. The calculated Strouhal number is

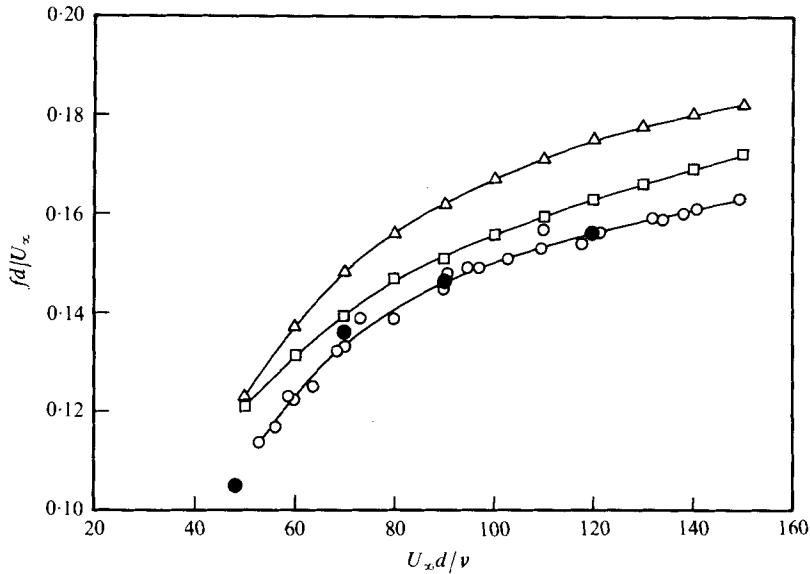


FIGURE 10. Strouhal number *vs.* Reynolds number. Experimental results: ○, present work; □, Berger & Wille; △, Roshko. Solid circles are values calculated with  $\beta_m = 0.48$  and experimental values of  $b/d$  at wake stagnation point.

shown in figure 10 by closed circles. The directly measured Strouhal number is shown by open circles. Results by Roshko (1954) and Berger & Wille (1972) are also shown. Calculated results agree very well with present experimental results. Thus we may state that the shedding frequency at Reynolds numbers between 48 and 70 is determined by the selective linear growth of small fluctuations.

At higher Reynolds numbers nonlinear effects are predominant. Because of the high growth rate at high Reynolds numbers, the amplitude of fluctuation becomes large in the standing eddies. Therefore, the eddies are deformed and the mean velocity distribution around the cylinder is modified. This in turn results in the change of frequency of the fluctuation of maximum growth rate. The actual process is not this kind of successive process. Both take place simultaneously and they cannot be separated. But if we take the measured velocity distribution at the stagnation point in the wake, the shedding frequency is predictable up to  $R = 120$  as shown in figure 10. The growth rates of natural fluctuations calculated from data in figure 5 are shown in figure 8(b) by triangles. They are compared with Nakaya's result at  $R_b = 40$ . Although theoretical results at higher Reynolds numbers are not available, the natural fluctuation seems to be the fluctuation with maximum growth rate. This fact has been found in various flow fields. At higher Reynolds numbers the region of growth of fluctuation moves upstream. It takes place at both sides of the cylinder and even in front of the cylinder. The mechanism of determining the shedding frequency is not clear in these cases because there is no distinct 'linear region'.

The effect of turbulence on the shedding frequency was discussed by Berger & Wille (1972). They found experimentally that the Strouhal numbers around

$$40 < R < 160$$

are different for different free-stream turbulence. This fact can be explained as follows. If the turbulence level is higher in the free stream, a high-intensity fluctuation

appears at smaller  $X$  and the nonlinear interaction also occurs at small  $X$ . The flow around the cylinder might be a little different from that with lower turbulence level in which nonlinear interaction takes place at larger  $X$ . This difference in the flow field around the cylinder results in different Strouhal numbers. It is not yet clear if this difference leads to two distinct families of Strouhal numbers as pointed out by Tritton (1959) and others.

## REFERENCES

- ACRIVOS, A., LEAL, L. G., SNOWDEN, D. D. & PAN, F. 1968 Further experiments on steady separated flows past bluff objects. *J. Fluid Mech.* **34**, 25.
- BERGER, E. & WILLE, R. 1972 Periodic flow phenomena. *Ann. Rev. Fluid Mech.* **4**, 313.
- DENNIS, S. C. R. & CHANG, G.-Z. 1970 Numerical solutions for steady flow past a circular cylinder at Reynolds numbers up to 100. *J. Fluid Mech.* **42**, 471.
- MATTINGLY, G. E. & CRIMINALE, W. O. 1972 The stability of an incompressible two-dimensional wake. *J. Fluid Mech.* **51**, 233.
- NAKAYA, C. 1976 Instability of the near wake behind a circular cylinder. *J. Phys. Soc. Japan* **41**, 1087.
- NISHIOKA, M. 1973 Hot-wire technique for measuring velocities at extremely low wind-speed. *Bull. Japan Soc. Mech. Engrs* **16**, 1887.
- NISHIOKA, M. & SATO, H. 1974 Measurements of velocity distributions in the wake of a circular cylinder at low Reynolds numbers. *J. Fluid Mech.* **65**, 97.
- ROSEKO, A. 1954 On the development of turbulent wakes from vortex streets. *N.A.C.A. Rep.* no. 1191.
- SATO, H. & KURIKI, K. 1961 The mechanism of transition in the wake of a thin flat plate placed parallel to a uniform flow. *J. Fluid Mech.* **11**, 321.
- TAKAMI, H. & KELLER, H. B. 1969 Steady two-dimensional viscous flow of an incompressible fluid past a circular cylinder. *Phys. Fluids Suppl.* **12**, II 51.
- TANEDA, S. 1956 Experimental investigation of the wakes behind cylinders and plates at low Reynolds numbers. *J. Phys. Soc. Japan* **11**, 1284.
- TRITTON, D. J. 1959 Experiments on the flow past a circular cylinder at low Reynolds numbers. *J. Fluid Mech.* **6**, 547.